

EVALUATION OF ASTER DATA USE IN LAND USE STUDY IN THE MEKONG DELTA

Pham Van Cu¹, Einar Lieng², Le Thanh Hoa³, Hiroshi Watanabe⁴
Hoang Kim Huong⁵

¹ *Centre for Applied Research in Remote Sensing and GIS, College of Science, VNU*

² *Norwegian Mapping Authority, Norway.*

³ *University of Social and Human Sciences of Ho Chi Minh City*

⁴ *Earth Remote Sensing Data Analysis Centre, Tokyo, Japan.*

⁵ *VTGEO, Institute of Geology, Vietnam Academy of Science and Technology*

ABSTRACT. The Mekong Delta in the south of Vietnam is a highly dynamic landscape with rapid changes in land use. Costal forests of mangrove (Rhizophoraceae, Sonneratiaceae and Avicenniaceae) and the more inland Melaleuca forests are changed into shrimp ponds and rice fields. The complex crop calendar and the diversification of land use types strongly influenced by the agriculture product market create a very complicated land use practice in the Mekong Delta. This increases costal erosion and gives a local rise in temperature. Human activities also increase the risk of forest fires, and corridors are therefore made to protect the remaining forests. Monitoring these changes accurately with a low cost is essential. Existing maps are inaccurate and not updated. ASTER data have a high spatial and radiometric resolution and can be acquired at a low cost. We seek a methodology to optimize differentiation between rice, grassland and forest, forest types, soil types and rice growth stages. Characteristics of each band, band combinations and band ratios are examined. Thermal channels are also used in these combinations to monitor human activities.

1. Introduction

Ca Mau Province in the Mekong Delta has experienced a tremendous change in land use in the last ten years. Forests and agricultural land have been transformed into shrimp farms. This has been a trend in several South-East Asian countries in the late 80's and early 90's, and it happened in Vietnam in the 90's. Environmental costs are very high when shrimp farms are located in mangrove area (Hazarika et al., 2000). Shrimp farms have impact on land, water, forest and fishery resources.

Landuse maps of Ca Mau Province from the 1990s are outdated, and efficient and inexpensive ways of mapping were sought by local administration. Forest stand parameters are needed, as well as accurate landuse classes. Satellite imagery can be used for such mapping (Phinn et al., 2000) with a sufficient accuracy. But ancillary data like detailed elevation model and aerial photographs were not available.

ASTER data are still not widely used, though they have costs and radiometric and spectral advantages. Hyperspectral analysis is promising to increase the

discrimination capacity of ASTER data in land use mapping of such a dynamic area as the Mekong Delta in Vietnam. Forest stand parameters should be possible to extract. A series of 8 scenes of ASTER of 2002 are used for this analysis. This is done in the framework of the collaboration between the Centre for Remote Sensing and Geomatics (VTGEO), the Forest Protection Department (FPD) of Vietnam, and the Earth Remote Sensing Data Analysis Centre (ERSDAC) of Japan.

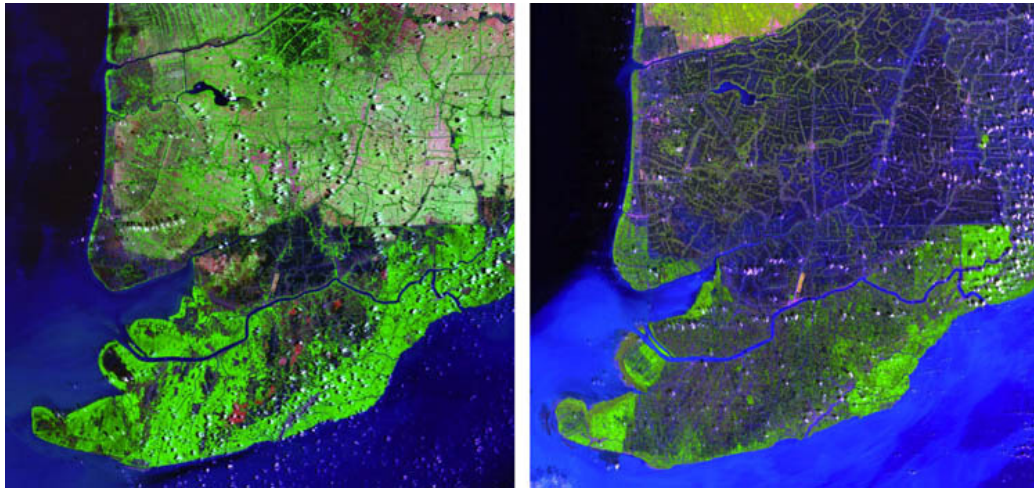


Figure 1. Left: Southern part of Ca Mau. Landsat image from 1993 (NASA mosaic).
Right: ASTER image mosaic (band 432) from 2002. The subsets are 65km wide.
Shrimp farms appear as dark blue, mangrove forests appear as green and agriculture - pink/green

2. Study Area



Figure 2. Location of Ca Mau Province

Ca Mau is the southernmost province in Vietnam and covers 5,200km², with a population of 1.1 million. The land is made of deposits from the Mekong Delta. Almost half of the area has been changed from forests and agriculture into shrimp farms in the last ten years. The coastline erodes at a rate of more than 100 meters per year in some areas.

In April 2002, there was a major forest fire in a Melaleuca forest reserve in Ca Mau. The Forest Protection Department (FPD) of Ca Mau is responsible for administrating the diminishing forests.

3. ASTER data, preparation and ground truth

The ASTER instrument has three sensors that cover three parts of the electromagnetic spectra. ASTER images were acquired in cooperation with ERSDAC in Japan. Acquisitions from the dry season (December to April) in the Mekong Delta are necessary to minimize cloud cover. However, this might not be optimal regarding the NDVI for vegetation mapping (Yang et al., 2001).

Table 1. Characteristics of ASTER sensors (Abrams et al., 2002)

Sub system	Band No.	Spectral Range (μm)	Spatial Resolution	Quant. Levels
VNIR	1	0.52 - 0.60	15 m	8 bits
	2	0.63 - 0.69		
	3N	0.78 - 0.86		
	3B	0.78 - 0.86		
SWIR	4	1.60 - 1.70	30 m	8 bits
	5	2.145 - 2.185		
	6	2.185 - 2.225		
	7	2.235 - 2.285		
	8	2.295 - 2.365		
	9	2.360 - 2.430		
TIR	10	8.125 - 8.475	90 m	12 bits
	11	8.475 - 8.825		
	12	8.925 - 9.275		
	13	10.25 - 10.95		
	14	10.95 - 11.65		

As the topography of Ca Mau is almost flat, geometric correction was performed without DEM. Available digitized vector data were of low geometric quality - about 50 meter standard deviation. Multitemporal analysis therefore was done with path oriented data. SWIR and TIR bands were resampled to VNIR resolution during georeferencing. There were no field measurements for K and C estimation for reflectance

conversion (Sonobe et al., 2002). The study was therefore performed with DN values. TIR values were converted from DN to temperature in degree Celsius with Planck's formula (Wantanabe, 2003). Multidate thermal bands were normalized with linear regression before mosaicking and change detection. TIR band 12 and green band thresholds were used to mask clouds for later analysis. Cloud masking is important for the spectral unmixing analysis.

Table 2. Image data

Dataset	ASTER acquisition	Date	Number of scenes
A	125/149-152	2002-01-12	4
B	126/149-152	2002-02-04	4
C	126/150-151	2003-01-06	2

A field excursion to Ca Mau was arranged in April 2003, at the day of ASTER acquisition over Ca Mau. No images were acquired due to overcast weather. Ground truths were collected in Melaleuca forest and costal mangrove forests.

4. Methodology

As the studied area is characterized by a large diversity of land use practice with a land cover of small size, the discrimination capacity of the data is essential. ASTER data with a spatial resolution even of 15m are still limited for the detailed land use mapping of the studied area. Instead of this, ASTER data provide a wide range of spectra and we assume that there exist some combinations of spectral bands in all three domains: VNIR, SWIR and TIR which may be the bests for land cover classification. Thus, the discrimination capacity of different band combinations is to be verified first for different types of land cover. These combinations will be used for the classification for the land cover types for which the combination is the most discriminative. Due to the constraints of the spatial resolution of ASTER data in terms of parcel size in the studied area, the physical indexes such as NDVI and VSW will be used to ameliorate the classification results.

5. Band combination analysis

To find optimal band combinations for forest, rice and soil discrimination, statistics from sample areas were evaluated. Band 7-14 show high degree of correlation.

Two test areas were chosen for test of classification methodology, a melaleuca and a mangrove subset. Each subset covers 161 km². Clouds were masked out. The images were classified using a supervised maximum likelihood classification. A classification scheme with an hierarchical class refinement was made for classification and accuracy

assessment. Seven easily distinguishable classes were chosen. Shadows, water, soil, rice, bush, young planted forest and fully grown forest. The class bush includes scrub, orchards and other trees than melaleuca and mangrove. Bands 1-6 were used for classification. The less correlated bands for vegetation mapping are band 2 and 3, while for water band 1 and 5 are the least correlated.

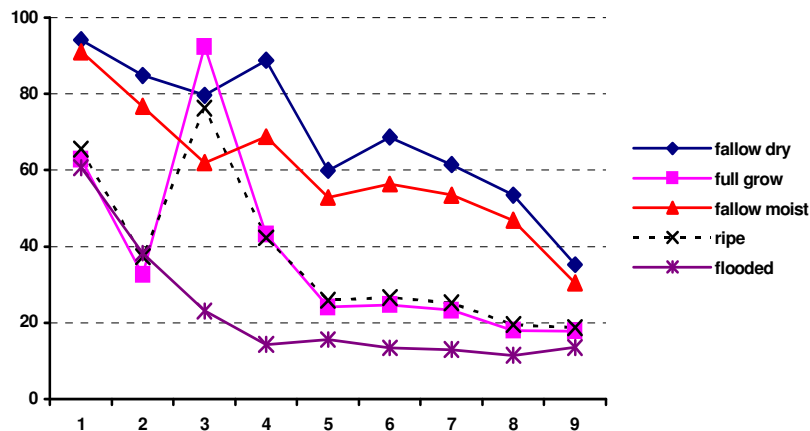


Figure 3. Spectral signatures for rice growth stages. Visible (1-3) and infrared bands (4-6), values in radiance. Full grow are often referred to as “heading”

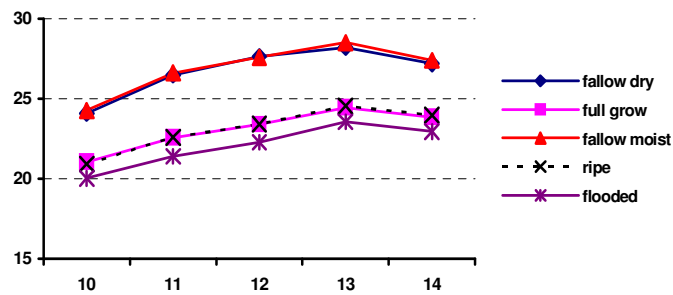


Figure 4. Spectral signatures for rice growth stages. Thermal bands (10-14), values in degrees Celsius

6. Classification using the best band combination

Table 3 shows the result of an accuracy assessment based on classification results with different channels and a digitized ground truth image. The ground truth image was made from screen digitizing the satellite image. This is not an optimal approach (Congalton and Green, 1999), but the digitizing was performed independently from training areas by a well trained person not involved in the classification. The accuracy of the ground truth image was found to be sufficient due to numerous ground truth samples and photos taken in the area on the 2003 fieldtrip.

Table 3. Melaleuca landuse classification, Producer's accuracy

	Band 1-3	Band 1-6	Band 2-4	Band 1-5	Band 1-4
Shadow	9.3 %	19.4 %	18.2 %	20.0 %	19.9 %
Water	73.1 %	70.6 %	64.7 %	70.3 %	68.2 %
Fallow	94.6 %	91.2 %	90.9 %	90.9 %	91.4 %
Grass	43.3 %	53.7 %	61.4 %	58.2 %	60.2 %
Bush	40.4 %	51.5 %	45.7 %	49.4 %	45.7 %
Young Melaleuca	58.4 %	55.9 %	55.0 %	56.0 %	55.0 %
Melaleuca	88.8 %	78.4 %	85.2 %	77.0 %	85.9 %
Overall Accuracy	61.4 %	65.0 %	65.9 %	66.0 %	66.3 %

Band combination 1-4 gives the best overall accuracy, while only the VNIR bands 1-3 can be more accurate for forest only. Confusion between bush and fallow fields appear within band 1-3. The rice and grassland confusion need to be solved with postclassification, as rice yields have numerous stages of growth. Rice mapping should be done with multitemporal images (Wahyunto et al., 2002).

Table 4. Melaleuca landuse classification. Confusion matrix (in %), band 1-4

	Water	Fallow	Grass	Bush	Y.Melale	Melale	Total
Water	68.2	0.4	0.2	1.6	0.1	0.0	14.1
Fallow	27.6	91.4	9.6	14.6	4.2	0.0	26.5
Grass	3.6	4.5	60.2	28.4	6.8	4.9	28.1
Bush	0.2	2.9	28.1	45.7	33.5	5.0	19.9
Young Melaleuca	0.4	0.7	1.7	9.3	55.1	4.1	4.6
Melaleuca	0.0	0.0	0.3	0.3	0.3	85.9	6.7
Total	100	100	100	100	100	100	100

7. Spectral unmixing

To find additional parameters like forest stand, spectral unmixing was performed. This can be done by collecting endmembers for areas of similar spectral variability (Smith et al., 1994). A simpler way of spectral mixture analysis is the VSW (vegetation-soil-water) index (Yamagata et al., 1997). Instead of using the VSW index for classification directly (ex. with segmentation and clustering, Crepani et al., 2002), post classification with VSW layers was preferred. Vegetation score was sliced into classes and overlaid with the classification result. This cross product enables a more refined classification product.

Melaleuca and mangrove are spectrally distinguishable, but a prestratification is preferred in order to separate younger and fully grown forests. Planted Melaleuca forests are inland and appear as homogeneous, dark and compact. Mangrove forests appear along the coastline and their natural or planted forest patterns (rows with channels) are recognizable. Except for some planted melaleucas in gardens, these two species have distinct habitats as melaleuca can not survive in saltwater and mangrove needs salt or brackish water.

Water score was sliced into two classes for separation between open water/sea and shallow water/shrimp/fish farms. The accuracy of adding water score was significantly better than adding vegetation score, which hardly gave any useful information. 200 randomly generated points were used for assessment.

Table 5. Mangrove classification accuracy. Vegetation and water score added

	Producer's Accuracy	User's Accuracy
Water (sea, channels)	83.3 %	88.9 %
Shrimppond, shallow	81.8 %	58.1 %
Soil, infrastructure	57.6 %	48.7 %
Mangrove open	7.1 %	25.0 %
Mangrove dense	92.0 %	71.9 %
Mangrove young	60.3 %	71.4 %
Overall Accuracy	68.0 %	

8. Classification applied for Ca Mau Province

Dataset A and B where each mosaicked and classified using band 1-4. A sea and cloud mask was made for Ca Mau and neighboring area using band 1, 3, 4, and 12. For statistics, the classified image was masked with administrative borders.

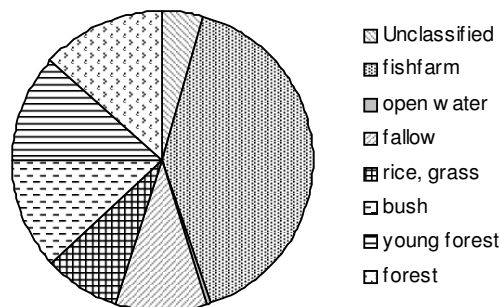


Figure 5. Land cover distribution Ca Mau Province

The whole province covers 5,213km², according to the dataset that was used. 4,977km² was classified as open water (channels, lakes), fish and shrimp farms, fallow soil and infrastructure, rice and grassland, bush, young forest and forest. Fish and shrimp farms were by far the biggest class covering about 40% or 2,092km². According to the confusion matrix, fishfarms are mainly confused spectrally with fallow soil. Unclassified area is sea and clouds.

9. Multitemporal analysis

The forest fire occurred in April 2002 was covered by dataset A before fire and C after fire. We wanted to find the change in the forest cover in the two datasets. The fire field had been regrown since the fire, mostly by reeds. Two approaches were chosen, a temperature change analysis and a post-classification analysis. Thermal bands might be used directly for change analysis and threshold since solar illumination is approximately constant in the flat landscape. However, images should be free of haze, as this absorbs thermal radiance. Spectral change analysis was not chosen due to the variety of spectral signatures.

A subset of 530km² was chosen for the study. Sea and clouds were masked out and 390km² were left. Forests (mainly melaleuca) were classified in each dataset using supervised maximum likelihood classification. 2002 forest cover was 118 km² and there was a decrease of 30km² or 25% in the next year. Lost forest cover is described as a change from forest or bush to non-forest (water-fallow-grass), the accuracy of this classification should be 70% (calculated from confusion matrix, Table 4).

Table 6. Forest cover change and temperature difference

Description	Area (ha)	%
Forest gained, >1°C temperature decrease	1104	2.8
No forest lost, >1°C temperature decrease	9032	23.2
No forest lost, +/-1°C temperature change	21354	54.7
No forest lost, 1-2°C temperature increase	3964	10.2
No forest lost, >2°C temperature increase	329	0.8
Forest lost, no temperature increase	1286	3.3
Forest lost, 1-2°C temperature increase	891	2.3
Forest lost, >2°C temperature increase	810	2.1
Total	39007	100

Table 6 describes the correlation between temperature change and forest cover change. A large fire field or clear-cut area creates a drastic increase in temperature,

from 3-8 degrees Celsius in the ASTER thermal bands. But surrounding areas tend to be heated up and borders are not very accurate. This explains the 0.8 percent of land where there is no forest lost but an increase of more than 2°C.

10. Conclusions

Band combination 1-4 gave the best result for supervised classification. Vegetation and water score made additional classes possible to refine, but only water score proved to be of accepted accuracy.

In the Ca Mau region, fish and shrimp farming have changed the landuse drastically over the last ten years. 40% of Ca Mau is now used as such farms.

The thermal bands can be used to make a quick change detection in forest cover. Change detection by classification is more accurate but labor intensive. Forest lost to clear cutting or forest fire had a temperature increase of more than 1°C in 57% of the cases. 71% of areas with a temperature increase more than 2°C had lost its forest cover.

With ASTER data, landuse changes like agriculture to shrimp farming and coastline movement are easily monitored. Planted forests are recognized and stand can be evaluated. Mixed forests and agriculture and grassland are difficult to interpret. Such areas might be delineated and studied further by multitemporal analysis.

Acknowledgements: This study is funded by ERSDAC and FPD Vietnam. Mr. Lieng's work was performed under Norwegian Fredskorps professional exchange program in the field of Geomatics. Mr. Watanabe from ERSDAC in Japan has provided us with ASTER images and advice on how to optimize the data use regarding the research topics. FPD in Ca Mau has assisted with ground truth information.

REFERENCES

- [1] Abrams, M., Hook, S., Ramachandran, B. (2002), *ASTER user handbook, version 2*. Jet Propulsion Laboratory / California Institute of Technology, USA.
- [2] Congalton, R. G., Green, K. (1999). *Assessing the accuracy of remotely sensed data: Principles and practices*. Lewis Publishers, USA.
- [3] Crepani, E., Duarte, V., Shimabukuro, Y.O. (2002), *Digital processing of Landsat-5 TM data for land use land cover regional mapping*. São José dos Campos, SP, Brasil
- [4] Hazarika, M.K. et al. (2000), Monitoring and impact of shrimp farming in the East coast of Thailand using Remote Sensing and GIS, *IAPRS*, Vol. XXXIII, Amsterdam.
- [5] Phinn, S. R. et al. (2000), Optimizing remotely sensed solutions for monitoring, modeling, and managing coastal environments. *Remote Sens. Environ.*, No 73, pp. 117–132.

- [6] Smith, M.O. et al. (1994), Imaging spectrometry - A tool for environmental observations. In: J. Hill and Mégier (eds.) *Spectral mixture analysis - new strategies for the analysis of multispectral data*. ECSC, EEC, EAEC, Brussels and Luxembourg, printed in the Netherlands, pp. 125-143.
- [7] Sonobe, T. et al. (2002), Utilization of ASTER data for wetland mapping of Kushiro Mire and Iriomote Island, Japan. In: Raghavan and Hoang (eds.) *International Symposium on GeoInformatics for Spatial-Infrastructure Development in Earth and Allied Sciences*. Hanoi, Vietnam, 25-28 September 2002, pp. 39-44.
- [8] Wahyunto, Widagdo and Abidin (2002), Rice yield estimation model in irrigated wetland rice areas of Java, Indonesia using Landsat TM data. *Asian Journal of Remote Sensing*, Vol. 3, No 2.
- [9] Wantanabe, H. (2003), *ASTER GDS Current Status*. ERSDAC, Japan.
- [10] Yamagata, Y., Sugita, S., and Yasuoka, Y. (1997), Development of Vegetation-Soil-Water Index algorithms and applications. *Japan Remote Sensing Journal*, 17(1), pp. 54-64 (in Japanese).
- [11] Yang, L. et al. (2001), *A Landsat 7 scene selection strategy for a National land cover database*. Raytheon ITSS, EROS Data Center, Sioux Falls, SD 57198 USA

